Trends in Biotechnology

CellPress OPEN ACCESS

Review

Advances and challenges in photosynthetic hydrogen production

Kevin E. Redding,[1] Jens Appel,[2] Marko Boehm,[2] Wolfgang Schuhmann,[3] Marc M. Nowaczyk,[4] Iftach Yacoby,[5] and Kirstin Gutekunst [2,*]

The vision to replace coal with hydrogen goes back to Jules Verne in 1874. However, sustainable hydrogen production remains challenging. The most elegant approach is to utilize photosynthesis for water splitting and to subsequently save solar energy as hydrogen. Cyanobacteria and green algae are unicellular photosynthetic organisms that contain hydrogenases and thereby possess the enzymatic equipment for photosynthetic hydrogen production. These features of cyanobacteria and algae have inspired artificial and semi-artificial *in vitro* techniques, that connect photoexcited materials or enzymes with hydrogenases or mimics of these for hydrogen production. These *in vitro* methods have on their part been models for the fusion of cyanobacterial and algal hydrogenases to photosynthetic photosystem I (PSI) *in vivo*, which recently succeeded as proofs of principle.

Highlights

Biotechnological solar hydrogen production has the aim to utilize electrons from the light reactions of photosynthesis. Recently, cyanobacterial and algal H_2ases, the enzymes that catalyze production of H_2, were successfully fused to PSI. They intercept electrons from the photosynthetic electron transport chain.

Both engineered strains produce photosynthetic hydrogen for prolonged periods. They maintained their ability to grow photoautotrophically.

The processes do not exclusively rely upon water oxidation as desired, which is mostly due to the fact that the H_2ases are sensitive to oxygen.

Cyanobacterial and algal photosynthetic hydrogen production

Biotechnological approaches for **photoH$_2$** (see Glossary) production aim to base the process on oxygenic photosynthesis. Water and sunlight are the only necessary ingredients to generate H_2 in this case. Two light-driven nanomachines [**photosystems I and II** (PSI and PSII)] (Figure 1) working in series propel electrons from water to the exact right potential to fuel hydrogen evolution. Compared to all other biotechnological options [1], this is the most direct and most efficient way. Since we think only the most efficient can compete with all the other sustainable energy sources this review article focuses especially on direct coupling of hydrogen production to photosynthesis, but we mention other approaches for comparison.

In the past, biological H_2 production has also been based on anoxygenic photosynthesis, that is, photosynthesis using electron donors other than water. We do not consider these options since they are not truly **sustainable**, as the electron donors used are neither abundant nor cheap enough for the scale required. The use of hydrogen as a fuel requires oxygen for its conversion to water. So, to close the circle, it is a must to generate H_2 from water, which leaves oxygen evolving (oxygenic) photosynthesis as the best option. This is especially challenging due to the oxygen sensitivity of most **hydrogenases** (H_2ases); the enzymes involved in H_2 formation.

Hydrogen production in cyanobacteria and algae driven by hydrogenases that could be directly linked to photosynthesis occurs under two conditions in **wild-type** (WT) strains. Under fermentative dark conditions, carbohydrates released from starch or glycogen are oxidized in a fermentative process, with H_2 as a byproduct. In contrast, photosynthetic H_2 production, which is performed by the same H_2ase, is a short-lived (up to a few minutes) process taking place at onset of illumination in anoxia. The H_2ases accept surplus electrons from the photosynthetic electron transport chain when the **Calvin–Benson–Bassham (CBB) cycle** is not activated [2,3]. Hence, it is functioning as an escape valve for surplus electrons before the CBB cycle gets running. Indeed, competing

[1]School of Molecular Sciences and Center for Bioenergy & Photosynthesis, Arizona State University, Tempe, AZ, USA
[2]Molecular Plant Physiology, Bioenergetics in Photoautotrophs, University Kassel, 34132 Kassel, Germany
[3]Analytical Chemistry – Center for Electrochemical Sciences (CES), Faculty of Chemistry and Biochemistry, Ruhr-University Bochum, Universitätsstrasse 150, 44780 Bochum, Germany
[4]Plant Biochemistry, Faculty of Biology and Biotechnology, Ruhr-University Bochum, Universitätsstrasse 150, D-44780 Bochum, Germany
[5]School of Plant Sciences and Food Security, The George S. Wise Faculty of Life Sciences, Tel-Aviv University, Ramat Aviv, 69978, Israel

*Correspondence: kirstin.gutekunst@uni-kassel.de (K. Gutekunst).

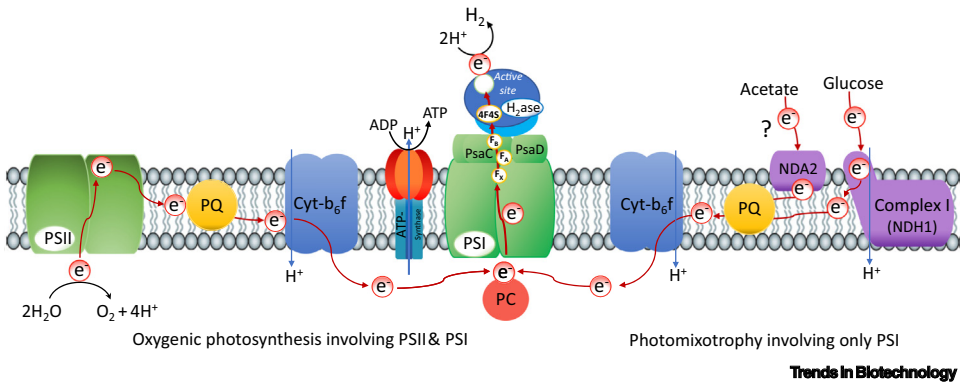

Figure 1. Hydrogenases (H_2ases) were genetically attached to photosystem (PS)I to intercept electrons for H_2 production. H_2 production was light driven both in the engineered cyanobacterial strain (PsaD–HoxYH) as well as in the engineered algal strain (ΨH1). The cyanobacterial NiFe-H_2ase HoxYH was fused to PSI subunit PsaD, whereas the algal FeFe-H_2ase HydA2 was inserted into the PSI subunit PsaC. H_2 production was partly driven by water oxidation at PSII as desired. In addition, glucose provided electrons for cyanobacterial photosynthetic H_2 production in the mutant strain. If acetate did likewise contribute to photoH_2 production in ΨH1 is unclear, as low PSI–HydA2 levels in relation to PSII kept the PQ pool reduced in this mutant.

processes (e.g., CO_2 fixation) are the reason for the fast cessation of hydrogen production [2,4,5]. Since H_2ases can also catalyze hydrogen oxidation, the hydrogen is eventually consumed after activation of the CBB cycle [3].

Another enzyme in cyanobacteria that is working as a hydrogenase is nitrogenase. Nitrogenases convert dinitrogen (N_2) to ammonia but inevitably produce one H_2 molecule per catalytic cycle [6]. If oxygen and nitrogen are removed from the cultures or if the uptake hydrogenase responsible to regain the reducing power of H_2 for the cells is deleted [7], specific cyanobaterial strains can produce H_2 for quite long periods [8]. The nitrogenase systems expends two ATP molecules per electron transferred, to drive down the potential sufficiently low to reduce N_2, rendering a high energetic cost of H_2 production (i.e., 16 ATP per H_2 under normal conditions, or as low as four ATP when N_2 is replaced with an inert gas). Thus, this process is not discussed further here.

Three different main classes of hydrogenases are known. [NiFe]-, [FeFe]- and [Fe]-hydrogenases. While [Fe]-hydrogenases are confined to methanogens, the first two classes are found in many different microorganisms and are each divided in a number of subclasses [9]. All known [FeFe]-enzymes are oxygen sensitive and need resynthesis of the enzyme or at least the active site metal cluster to become active again, whereas all [NiFe]-hydrogenases can be reactivated in the absence of oxygen and some, the so-called O_2-tolerant enzymes, are even able to work in the presence of ambient oxygen concentrations [10].

Recently, major steps have been achieved in a cyanobacterium and alga to enable biological hydrogen production from sunlight and water. In one representative of each group, a direct coupling of the hydrogenase to photosynthesis by fusion of the enzyme to PSI was accomplished that allowed sustained H_2 generation *in vivo* in the light. Here, we give an overview and a comparison of these studies, describe the different approaches and discuss the crucial obstacles that still need to be overcome for a sustained biotechnological application. We also give a short glimpse on recent *in vitro* attempts. The *in vivo* generation of photosystem–hydrogenase fusions might also boost these approaches and both might mutually benefit from each other since semiartifical systems could easily separate oxygen evolving PSII from H_2 evolving PSI in different half-cells.

Glossary

Calvin–Benson–Bassham cycle: CO_2-fixing cycle found in photoautotrophic cyanobacteria, algae, and plants.

Diaphorase: the cyanobacterial [NiFe] hydrogenase is composed of the diaphorase subunits HoxEFU which transfer electrons between electron donors as ferredoxin and NAD(P)H to/from the hydrogenase part composed of subunits HoxYH.

F_B-cluster: 4Fe4S cluster within PSI, which donates electrons to ferredoxin in WT strains.

Ferredoxin: small proteins that contain FeS clusters and shuttle electrons between reaction partners in redox reactions.

Flavodoxin: replaces ferredoxins under iron depletion and contains FMN instead of FeS clusters.

Hydrogenases: enzymes that catalyze the reduction of protons (H^+) to hydrogen (H_2) and vice versa. They differ in their subunit composition and in their active site metal clusters. The cyanobacterial bidirectional [NiFe] H_2ase is composed of five subunits HoxEFUYH, the cyanobacterial uptake hydrogenase is composed of two subunits HupSL, whereas the algal [FeFe] H_2ase is a monomeric enzyme made up of the single subunit HydA.

Maturases: auxiliary proteins required for the proper assembly of the active sites of H_2ases.

Oxygenic photosynthesis: photosynthesis as known from plants in which PSII and PSI are involved. The electron donor is water, which is split at PSII generating O_2.

PhotoH_2: hydrogen that is produced using electrons from the light-driven electron transport chain in thylakoid membranes.

Photomixotrophy: organisms require a source of energy and carbon. Photoautotrophs utilize light as energy source and CO_2 as carbon source. Photoheterotrophs utilize organic carbon instead of CO_2 and photomixotrophs utilize both CO_2 and organic carbon.

Photosystems I and II: the light reactions of photosynthesis take place in the thylakoid membranes of cyanobacteria, algae and plants. PSII and PSI are central complexes in which electrons are excited by light. They contain a reaction center with a special chlorophyll-a pair and antenna

Enzymatic properties

We focus on the bidirectional cyanobacterial [NiFe]-hydrogenase and the algal [FeFe]-hydrogenase, since they are convenient for hydrogen production. Both, the cyanobacterial and algal H_2ases accept electrons from **ferredoxin** (Fdx), which is reduced by PSI [11,12]. See Table 1 for a comparison of these two enzymes.

Both H_2ases are sensitive to O_2, although to different extents. The active site of cyanobacterial [NiFe]-H_2ases can be reactivated within seconds upon exposure to anoxic conditions [13]. [NiFe]-H_2ases probably reduce the bound oxygen to water [14,15]. The [FeFe]-H_2ases can be reactivated by insertion of a newly formed di-iron cluster into the damaged site by the **maturase** enzymes [16]. Although this process can take hours *in vitro*, it may happen much faster *in vivo* [16]. The algal [FeFe]-H_2ase is a monomeric enzyme made up of the subunit HydA while the [NiFe]-enzyme is made up of a small and a large subunit (HoxYH).

Table 1. Comparison of properties of the two systems discussed

	Chlamydomonas rheinhardtii	*Synechocystis* sp. PCC 6803
Type of H_2ase	[FeFe]-H_2ase [9]	[NiFe]-H_2ase [9]
Gene names	*hydA2* (monomeric enzyme)	*hoxYH* (dimeric enzyme)
Oxygen sensitivity	Sensitive [17]	Sensitive, but continues to evolve H_2 in the presence of low O_2 concentrations [13]
Reactivation after oxygen exposure	Needs protein resynthesis or at least resynthesis of active site metal cluster [16]	Is reactivated in seconds probably by releasing bound oxygen as water [13,15]
k_{cat} for H_2 evolution	~10^4 H_2/s [17]	1000–2000 H_2/s [18]
Highest *in-vivo* rates of electron flow through PSI	Not determined	72 e^-/s = 36 H_2/s [47]
Highest rates of photoH_2 production recorded of native enzyme	150 µmol H_2/mg Chl/h [2]	640 µmol H_2/mg Chl/h [18]
Natural electron donor for H_2 evolution	Ferredoxin	Ferredoxin [12]
Properties of PSI–H_2ase fusions		
Name of PSI–H_2ase fusion strain	ΨH1 [37]	*psaD-hoxYH* [36]
PSI subunit used for fusion construct	Inframe insertion into PsaC [37]	C-terminal fusion to truncated clamp of PsaD [36]
Distance between F_B cluster of PsaC and metal cluster in the H_2ase	15 Å [37]	23–45 Å [36]
Electron transfer from PSI to H_2ase	Not limiting [37]	Limiting [36]
In vivo level of PSI–H2ase compared to WT PSI	~15% [37]	~0.2% [18,36]
Rates of immediate PhotoH_2 production of fusion strains	120 µmol H_2/mg Chl/h [37]	0.5 µmol H_2/mg Chl/h [36]
Maximal immediate *in vivo* rates per PSI-H_2ase chimera	170 H_2/s [37]	~6 H_2/s [18,36]
Rates of long-term PhotoH_2 production of fusion strains	21 µmol H_2/mg Chl/h [37]	0.6 µmol H_2/mg Chl/h [36]
Major future challenge	Overcome oxygen sensitivity	Optimize electron transfer from PSI to the H_2ase

complexes with additional pigments (chlorophyll-a, chlorophyll-b, and carotenoids) to harvest light.
Phycobilisomes: cyanobacteria contain special antenna complexes that contain phycocyanin and/or phycoerythrin, which absorb light in the so-called green gap of chlorophylls and carotenoids.
PsaC: subunit of PSI containing terminal 4Fe4S clusters F_A and F_B.
PsaD: extrinsic subunit of PSI neighboring PsaC.
Sustainable hydrogen production: photosynthetic H_2 production is sustainable if it is exclusively based on water oxidation at PSII and driven by light. In this case, water is split into oxygen and electrons and light is the energy source that excites these electrons such that they can be utilized for H_2 production. H_2 can be subsequently combined in fuel cells with oxygen to liberate energy and reconstitute water in the so-called Knallgas reaction.
Wild type: natural strains that have not been manipulated genetically in contrast to mutant strains.

Hydrogen production rates of algal [FeFe]-H_2ases *in vitro* are ~10^4 H_2/s; nearly an order of magnitude higher than typical values for cyanobacterial [NiFe]-H_2ases (1000–2000 H_2/s) [17,18]. The *in vivo* rates are lower, as they are limited by electron input. Under irradiance of ~800 µE, the cyanobacterial enzyme can reach up to 640 µmol H_2/mg Chl/h [19] for about 10 s. For algal strains instantaneous rates of 100–200 µmol H_2/mg Chl/h are typically measured, and under some circumstances, even 450 µmol H_2/mg Chl/h have been found [20]. The maximal rate also lasts for about 10 s. Please note that the chlorophyll content is higher in algal cells.

Physiological approaches to enhance photosynthetic hydrogen production

There are several processes that compete with the H_2ases for reduced Fdx. Different physiological approaches have been taken to understand and enhance photosynthetic hydrogen production. These approaches are described briefly.

The green alga *Chlamydomonas reinhardtii* can be cultivated under sulfur deprivation to achieve hypoxic conditions in the light. Sulfur deficiency impairs the PSII repair cycle, which eventually results in lowered water splitting and continuous photoH_2 production [21]. The electrons for photoH_2 under these conditions originate from acetate and other carbon sources (e.g., starch), which are fed into the photosynthetic electron transport chain. The deletion of components of the cyclic electron flow around PSI increases the stability of PSII under sulfur deprivation and increases respiration, which further enhances photoH_2 production [22]. Another approach is to cultivate green algae at low light on acetate in order to balance photosynthesis and respiration such that oxygen does not accumulate [23]; unfortunately, this lowers the H_2 photoproduction rate. The electrons for continuous photoH_2 production originate from a mixture of water oxidation, acetate and photofermentation of proteins. However, the major drawback of these processes is that they are not carbon neutral. In addition, sulfur deprivation requires two light absorbing phases. A first phase to fix carbon and a second phase fed by the breakdown of the previously generated carbon skeletons, which reduces the conversion efficiency of sun light to H_2, let alone the energy needed to exchange the media.

Another route to bypass the sulfur deprivation is to fuse the H_2ases to strategic hotspots in the photosynthetic apparatus, which allows it to obtain a prolonged electron supply. For example, fusing H_2ases to the enzyme superoxide reductase, which binds to the photosynthetic machinery, allows continuous photoH_2 production for longer than 12 days at rates of 4.5 µmol H_2/mg Chl/h [24].

The second hurdle for photoH_2 production are the processes that compete for reduced Fdx and thereby reduce H_2 production. The main competitor is the CBB cycle, which oxidizes NADPH provided via ferredoxin–$NADP^+$ reductase (FNR). FNR likely has a competitive advantage over other downstream electron acceptors due to its binding to the PSI acceptor side [25]. PetF (ferredoxin 1) is the major Fdx in *C. rheinhardtii*. It contains two aspartic acid residues that are crucial for the differential recognition of FNR and HYDA1. The replacement of these residues with alanine represses FNR binding, which results in a reduced electron flow to CO_2 fixation and increased photoH_2 production *in vitro* [26]. PhotoH_2 production in the cyanobacterium *Synechocystis* sp. PCC 6803 is likewise enhanced and prolonged by partial deletion of FNR [12]. Mutation of specific residues in the cyanobacterial FNR and ferredoxin also results in higher electron transfer rates to algal HydA *in vitro* [27]. Fusion of PetF to HYDA1 diverts the electron flow to the H_2ase *in vitro* and *in vivo* and enhances as a side effect its resistance to oxygen [28,29]. The fusion protein is able to intercept photosynthetic electrons and yields elevated photoH_2 production rates. Continuous photoH_2 production in the green algae is achieved by keeping the CBB cycle inactive under anoxic conditions in the light. This can be accomplished by limitation of its substrate CO_2 or by a train of short light pulses of 1 s that alternate with 9 s darkness [4,30].

The CBB cycle is inactive in darkness and intermittent short light pulses of this length do not suffice for its activation. For both approaches electrons for photoH_2 production originate primarily from water oxidation at PSII [5,30]. Nitrate assimilation and respiratory oxidases that fine-tune photosynthesis are further competitors for photoH_2 production in cyanobacteria. Inhibition of nitrate assimilation and deletion of respiratory oxidases have been shown to enhance photoH_2 production in the cyanobacterium *Synechocystis sp. PCC6803* [19].

Another process competing with photoH_2 is photoreduction of O_2 (Mehler reaction), albeit at lower levels compared to the CBB cycle. This was shown for algal mutants without the flavodiiron (Flv) protein that is responsible for this reaction [31,32].

H_2 production in heterocysts

Some nitrogen-fixing filamentous cyanobacteria form specialized cells, so called heterocysts, under nitrogen deprivation. Heterocysts have thicker cell walls than neighboring vegetative cells, lack PSII, and show increased respiratory activity, which results in micro-oxic conditions to protect oxygen-sensitive nitrogenases [33]. The electrons for N_2-fixation are derived from Fdx that was reduced by PSI. Clostridial [FeFe] H_2ases expressed in cyanobacterial heterocysts are able to intercept photosynthetic electrons before reaching the nitrogenase and yield enhanced amounts of hydrogen at rates that are above those of the parent strain [34]. However, the [FeFe]-Hase turned out to be more oxygen sensitive than the nitrogenase and to be inactivated even in the heterocysts. Overproduction of Flv3B was shown to increase heterocystous H_2 production probably by enhanced O_2 consumption [35] and could also help when expressing [FeFe]-H_2ases. However, since heterocystous H_2 production requires CO_2 fixation in vegetative cells first, then translocation of the carbon skeleton to the heterocysts followed by break down and another light absorbing event to get the electrons to the level of H_2 it is less efficient than direct water oxidation.

In vivo fusion of hydrogenases to PSI in cyanobacteria and green algae

An approach to bypass the dependency on Fdx and gain a superior competitiveness with downstream processes, is to fuse the H_2ases to PSI *in vivo*. This is the most direct approach to enhance and prolong photoH_2 production in cyanobacteria and algae. Indeed, a proof of concept was achieved both in the cyanobacterium *Synechocystis sp.* PCC 6803 and in the green algae *Chlamydomonas reinhardtii* (Figure 1) [36,37]. We thus have the unique opportunity to compare the physiology and performance of a unicellular prokaryotic with a unicellular eukaryotic photosynthetic organism that have H_2ases directly attached to their PSIs. For a reflection on the possible solar to hydrogen conversion efficiency of the whole process see Box 1 and for a comparison of the two systems see Table 1.

Design and function of PSI-H_2ase chimeric proteins

The FeS clusters of PSI and the H_2ases must be placed within distances that allow efficient electron transfer (Box 2). The aim of both approaches was to intercept electrons from the **F_B cluster** of the **PsaC subunit** of PSI (Figure 2). The different structures of the H_2ases necessitated the use of different anchors to PSI. The C terminus of **PsaD** passes over PsaC in proximity to the F_B cluster and then binds to the surface of PsaB. This C-terminal clamp is thought to contribute to the tight association of PsaC with PSI [38]. The small subunit (HoxY) of the [NiFe]-H_2ase is attached to a truncated version of the PsaD clamp in cyanobacterial PSI and its association with HoxH is counted upon to assemble PSI–HoxYH. This is referred to as the PsaD–HoxYH fusion and the cyanobacterial mutant as *psaD–hoxYH* (Figures 1 and 2).

The PsaC subunit possesses a β-hairpin that is located on top of the F_B cluster and forms part of the Fdx-binding site (Figure 2). The algal H_2ase domain HydA2 was inserted as an inframe fusion

Box 1. Solar to hydrogen conversion efficiency

Although existing systems do not yet fulfill the requirements for a successful application, here is a short and rough reflection on their potential efficiency. Photosynthesis is predominantly driven by blue and red light absorbed by the two photosystems (PSII and PSI) (see Figure I in Box 3). The energy of one mole of red photons of the wavelength 680 nm is:

$$E = h \times \frac{c}{\lambda} \times N_A = 6.63 \times 10^{-34} \times \frac{2.99 \times 10^{8}}{680 \times 10^{-9}} \times 6.02 \times 10^{23} = 176\ \text{kJ/mol}$$

The energy of combustion of hydrogen is 286 kJ/mol. Since two electrons need to be driven along the whole chain to reduce two protons to H_2, four photons are required. Thus, 704 kJ of red radiation need to be invested, yielding a maximum efficiency of 286/704 × 100 = 41%. This seems impressive.

However, there are flaws in this calculation. First, no matter which photon the photosystems absorb, its energy is ultimately reduced to that of a red photon and the rest will be given off as heat. Second, not every absorption of a photon leads to a successful charge separation. If we incorporate the photochemical efficiency of the photosystems, the number of photons required would increase to 4.4 instead of 4. Taking the absorption spectrum of green algae into account that is close to that of chlorophyll a (Figure I), we obtained a conversion efficiency of 3.1% and for cyanobacteria that contain **phycobilisomes** (efficient light harvesting complexes) about 5.8%. *In vivo* the quantum requirement for the production of one O_2 is between 10 and 11 instead of the theoretical eight [47,54], because additional energy is needed for CO_2 uptake, and cellular maintenance and repair. CO_2 uptake is not of concern when the cells produce H_2 but maintenance and repair, especially of the photosystems, are necessary. This increases the quantum requirement to about 5.5 per H_2 and decreases the theoretically attainable conversion efficiency of algae to 2.5% and of cyanobacteria to 4.6%. These calculations hold for a single cell layer. If we imagine denser cultures these values increase because a larger proportion of the light can be absorbed. If we maintain the above quantum requirement of 5.5 per H_2 and imagine that every photon of the whole spectrum up to 710 nm could be used, the solar to hydrogen conversion efficiency could be estimated to get to about 13.5% at its best [55].

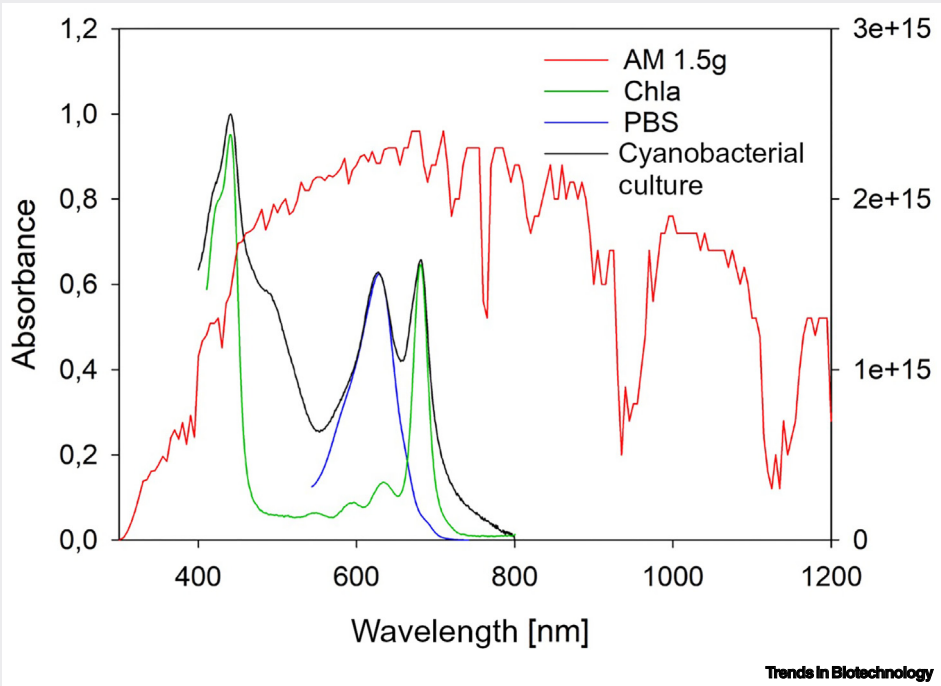

Figure I. The standard solar spectrum AM 1.5g at a zenith angle of 48.5° that is used to determine the efficiency of photovoltaic devices and the absorption spectra of chlorophyll a, the cyanobacterial phycobilisome (PBS) and a cyanobacterial culture. These spectra have been used for the calculation of potential efficiencies above.

Box 2. Electron transfer within PSI and to H_2ases

Charge separation within PSI occurs after excitation energy has arrived at the six coupled chlorophylls in the electron transfer domain at the center of PSI, typically from the surrounding antenna domains (containing ~90 chlorophylls). In addition, cyanobacteria contain phycobilisomes and IsiA antenna polypeptides, while green algae have light-harvesting I complexes, which further increase the number of antenna pigments connected to PSI. Initial charge separation is thought to occur between the ec2 and ec3 Chls within ~1 ps, generating the $ec2^{+}ec3^{-}$ radical pair state, followed by hole transfer to the P_{700} Chl dimer and electron transfer to the nearby phylloquinone in 20–50 ps, generating the P_{700}^{+} PhQ^{-} state (see Figure 2 in main text). Work on algal and cyanobacterial PSI have shown that both electron transfer branches are active for charge separation, with the A-branch somewhat dominant, being used 55–75% of the time [56,57]. Electron transfer to the F_X cluster occurs in ~20 ns from the B-side semiquinone and in ~200 ns from the A-side semiquinone. This is followed by transfer to the F_A/F_B clusters of PsaC in ~140 ns [58].

In the absence of electron acceptors for the FeS clusters, charge recombination with P_{700}^{+} occurs in ~100 ms from $(F_A/F_B)^{-}$ and in ~0.5 ms from F_X^{-}. This is why electron transfer to the attached H_2ase must be reasonably fast (<10 ms), in order to compete with the back reaction. The Moser-Dutton approximation [59] relates the rate of electron transfer (k_{ET}) to the distance between the cofactors (R, in Å), the driving force of the reaction (ΔG) and the reorganization energy (λ):

$$\log k_{ET} = 13 - (\beta/2.3)(R - 3.6) - (\gamma/\lambda)(G + \lambda)^2$$

The maximum rate (i.e., when ΔG = -λ) can be easily calculated, assuming an average β of 1.4/Å for electron transfer within proteins as $k_{ET} = 10^{(15.2 - 0.61R)}/s$.

There is insufficient data to estimate the other parameters for this electron transfer event in the two chimeric assemblies. While the link in PsaD–HoxYH is assumed to be rather flexible, PsaC–HydA2 can be modeled as a new protein resembling a clostridial hydrogenase with a Fdx-like domain harboring supplementary FeS clusters [60]. This could mean that the actual electron transfer rate would be further from optimality in PSI–HoxYH than in PSI–HydA2, due to a higher expected reorganization energy in the former because of its more polar environment, but there are too many unknowns to state this with any confidence.

into the loop of this β-hairpin, splitting PsaC into two short polypeptides that have to assemble together after folding of the HydA domain. This polypeptide is termed PsaC–HydA2 and the chimeric complex is PSI–HydA2. This resulted in the algal mutant ΨH1 (Figures 1 and 2).

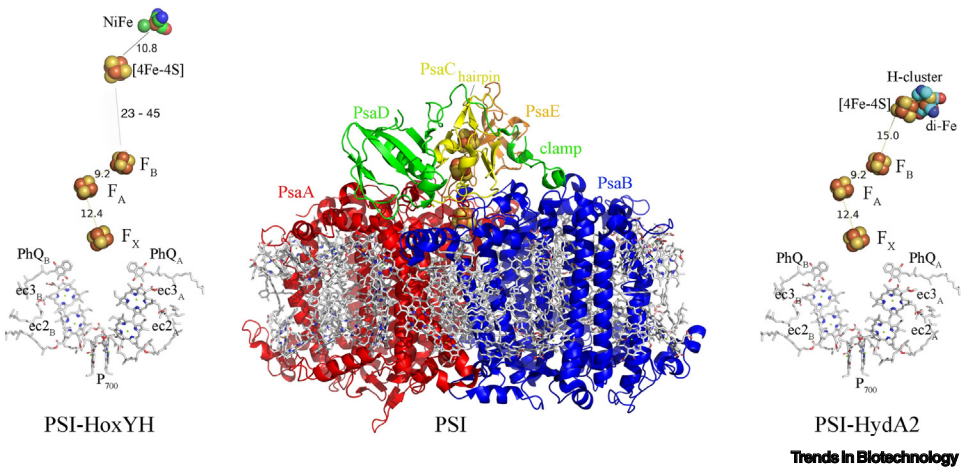

Figure 2. The arrangement of subunits within photosystem (PS)I is shown in the center. The PsaA/B heterodimer in the membrane binds all of the chlorophylls of the antenna domains (~90) and the six electron transfer chlorophylls at the center, as well as the PhQ and F_X cofactors. PsaC binds the terminal F_A and F_B clusters. PsaD participates in binding Fdx and its C-terminal clamp extends over PsaC. The β-hairpin insertion site for HydA in PsaC is also indicated. On the left and right are shown the arrangement of cofactors within PSI and the attached hydrogenases, with distances between metallic clusters (in Å) noted. PDB files used: PSI (1JB0), [NiFe] H_2ase (5xf9), HydA1 (4R0V).

In both cases, the chimeric polypeptides (PsaD–HoxYH and PsaC–HydA2) have been shown to assemble into a complex with the other PSI subunits, as shown by immunoblot analysis on 2D gels (PSI–HoxYH) or of purified protein (PSI–HydA2). Moreover, the hydrogenase moiety of each complex appeared to be fully active as judged by using reduced methyl viologen as electron donor for H_2 production. This proves that maturation of the H_2ase domain works in both mutants, even when attached to PSI. The question is whether PSI is an effective donor to the attached H_2ase. Both engineered strains produce photoH_2 in a light-dependent manner. In order to compete effectively with charge recombination of the $P_{700}^{+}(F_A/F_B)^{-}$ state (in ~100 ms), electron transfer from F_B to the H_2ase active site should be significantly faster than that. Using the Moser–Dutton ruler approximation [39], an electron transfer time of 1 or 10 ms (~99% or ~90% yield) would require a maximum distance of 20 Å or 21.6 Å. The calculated distances between F_B of PSI and the 4Fe-4S cluster of HoxY or HydA2 are 23.3–45.2 Å or 14.8 Å, respectively, based upon reasonable models (Figure 2, Box 2).

Effect of PSI–H_2ases on physiology

The PsaC and PsaD subunits interact intimately in PSI, which means that the [NiFe]-H_2ase would be close to the F_B cluster but also posed a risk that the added H_2ase could compromise proper PSI assembly. This is visible by a reduced PsaC level in the PSI–HoxYH expressing strain. In the ΨH1 strain the PsaD level is similar, but the level of the chimera was reduced about eightfold compared to WT PSI. This is likely due to the demanding nature of the chimeric design, requiring the two halves of PsaC to assemble together properly, followed by binding of the PsaC domain to newly assembled PsaA/PsaB heterodimer in the thylakoid membrane. In the absence of PsaC in *C. reinhardtii*, there is little detectable PSI, due to coordinated degradation of the unassembled subunits [40]. Thus, the PsaC domain of the PsaC–HydA2 polypeptide either folds less efficiently or binds less well to PSI.

In both cases, the PSI–H_2ase chimera replaces normal PSI and still allows photoautotrophic growth, albeit at low rates, indicating that they were able to reduce Fdx. In the case of the ΨH1, photoautotrophic growth takes place only under micro-oxic, high-CO_2 conditions; this phenotype was previously seen with mutant strains containing similar low amounts of PSI [41].

In PSI–HydA2, the Fdx binding site on PsaC should have been blocked. As expected, the photoreduction of cyanobacterial **flavodoxin** *in vitro* was reduced by an order of magnitude [37], consistent with the fact that its binding site heavily overlaps the Fdx binding site [42]. However, Fdx photoreduction was only lowered twofold. The explanation given for these observations was that the 4Fe-4S cluster of the HydA2 domain (which exists before insertion of the di-iron subsite) was the actual reductant of Fdx, given that the Fdx binding site of HydA2 was not blocked in the chimera.

In vivo hydrogen production by PSI–H_2ases

Since PSI–HydA2 maintains its ability to interact with Fdx, it is not surprising that the respective strain is capable of fermentative H_2 production in the dark (at 60% the WT level, consistent with total cellular H_2ase activity). In contrast, the PSI–HoxYH expressing mutant lacks this capability, as HoxYH alone cannot interact with its electron donor/acceptor due to the lack of the **diaphorase** HoxEFU.

In both systems, the engineered cells performed photoH_2 production after anaerobic dark–light transition. The maximal transient rate of PsaD–hoxYH was 0.5 µmol H_2/(mg Chl h)$^{-1}$, which is less than the WT (14 µmol H_2/mg Chl/h). Only about 0.2% of the PSI centers have a H_2ase, which gives about 6 H_2/s per PSI–HoxYH chimera, and indicates that the electron transfer from

PSI to hydrogen is far from optimal in this case. The maximal transient rate estimated for the ΨH1 strain under imposed anoxia (with glucose oxidase) is 120 µmol H_2/mg Chl/h)$^-$, or 2.7 mmol H_2/g dry cells/h, which is an order of magnitude higher than that measured in the WT strain. This is equivalent to ~170 molecules of H_2/s for each PSI–HydA2 (assuming that all are active at steady state), which puts a lower limit on the k_{cat} of PSI–HydA2. This rate compares favorably to a chimera in which cyanobacterial PSI is linked to clostridial [FeFe]-H_2ase via a molecular wire, which produced ~50 H_2/s *in vitro* [72]. In both cases it is likely electron input into PSI that limits the overall rate of H_2 production. A telling difference between photoH_2 production in the PSI–HydA2 and WT strains is the light saturation curve, with PSI–HydA2 requiring higher light than WT (half saturation at 300–500 vs. <50 µmol photons/m^2/s) to achieve a rate saturating at a value ~8-fold higher than WT. This was explained by the ability of the HydA2 domain to transfer an electron to Fdx, inhibiting photoH_2 production at low light, when the delay between delivery of the first and second electron would be longer.

Both engineered strains produce photoH_2 for several hours under anaerobic conditions (PSI–HoxYH strain: 0.6 µmol H_2/mg Chl/h), ΨH1: 21 µmol H_2/mg Chl/h). In WT green algae and cyanobacteria, the onset of CO_2 fixation terminates photoH_2 production within several minutes. However, ΨH1 continues to produce photoH_2 due to the diversion of most electrons to H_2 production away from CO_2 fixation. In addition, the ΨH1 cultures did not accumulate O_2 due to the low amount of PSI–HydA2 constraining O_2 production by PSII. During the long-term photoH_2 production experiments over the course of days, glucose was added to *psaD–hoxYH* cultures and acetate was added to ΨH1 cultures (Figure 1). The ΨH1 strain produced H_2 at ~14 µmol H_2/mg Chl/h) as a dilute culture in a sealed bottle or ~5 µmol H_2/mg Chl/h as a dense culture in a photobioreactor over the course of several days. The *psaD–hoxYH* strain performed long-term photoH_2 production at a rate of 0.6 µmol H_2/mg Chl/h while H_2 production by WT cyanobacteria is barely detectable under the same circumstances.

Several points are relevant to the discussion of long-term photoH_2 production in the engineered strains. Firstly, it is light dependent, as expected. Secondly, it is based on electrons coming from H_2O splitting at PSII, as desired, but may utilize electrons from organic donors (e.g., starch, glycogen, glucose, or acetate) as well. In the case of the ΨH1 strain, such donors are required to drive respiration to maintain anaerobiosis, but they likely do not contribute directly to proton reduction, as the plastoquinone pool (where electrons from such sources enter the electron transport chain) is highly reduced in bright light due to the high PSII/PSI ratio. The processes are thus driven by a mix of **photomixotrophy** involving only PSI and photoautotrophy based on **oxygenic photosynthesis**, water splitting, PSII, and PSI (Figure 1). The ratio of these sources depends upon the system in use. Thirdly, despite the claims that the algal [FeFe]-H_2ase is 'exquisitely sensitive' to O_2, being irreversibly inactivated within 1 s of O_2 exposure, long-term photoH_2 production by PSI–HydA2 in the face of constant O_2 evolution by PSII in the same membrane could be a hint that this might not be such a serious problem. This adds support to the idea that the so-called HydEFG maturases are not solely involved in biosynthesis of new [FeFe]-H_2ase, but can also reactivate damaged enzyme, as has been shown *in vitro* [16]. Thus, there are real advantages to maintaining the PSI–H_2ase chimera in a cellular setting.

In vitro approaches, recent advances

Photosynthetic hydrogen production in cyanobacteria and green algae has inspired artificial and semiartificial approaches that mimic photosynthetic energy conversion for solar H_2 production *in vitro* (Box 3). Biohybrid approaches in which photosystems and/or enzymes are attached to electrodes or other materials have been studied in the last two decades. In this respect two studies using separately purified PSI and H_2ase to assemble PSI–H_2ase complexes are interesting [43,44].

Box 3. *In vitro* approaches, recent advances

Isolated photosynthetic protein complexes like PSI and PSII can be coupled in semiartificial, photoelectrochemical cells to mimic light-driven linear electron flow *in vitro* (Figure I) [61,62]. Electrons being released from water by PSII in the anodic half-cell are transferred to the PSI-containing cathodic half-cell [63] and passed to a catalyst (e.g., hydrogenase) to produce a fuel at the end of the chain [64].

One key point for optimization is the electrical connection between the biological components and the electrode, which is part of the individual half-cells in the electrochemical system. This can be either mediated by diffusible redox mediators [65] or achieved by oriented immobilization of redox-active proteins, which is usually supported by a self-assembled monolayer on the electrode surface [66]. Alternatively, oriented protein monolayers can be deposited on an electrode by the Langmuir–Blodgett technique [64,67]. Further improvement was achieved by application of redox-active hydrogels, which enable diffusion-free electron transfer between the protein and the electrode [68]. Here, proteins are embedded in a polymer film and wired to the electrode via redox-active groups (e.g., osmium bipyridine complexes, viologens, or phenothiazine-based dyes) attached to the polymer backbone. In principle, this setup also allows the integration of engineered photosystems to increase the light conversion efficiency, as considerable energy losses within the complexes are a direct consequence of diffusion dependent electron transfer processes in the native system.

Several concepts have been realized to achieve light-driven hydrogen production with biohybrid systems. For example, hydrogen was generated with platinum-nanoparticle-modified PSI complexes, which were embedded within a redox-active hydrogel as electron donor [69]. Integration of a hydrogenase into the photocathode is more challenging due to charge recombination between the PSI donor and acceptor side and, as a consequence, electron transfer to the hydrogenase must be insulated. This was achieved by a sandwich structure of several polymer–protein layers including PSI and hydrogenase [64]. Alternatively, a PSII-based photoanode was coupled to a hydrogenase containing cathode, either by applying an additional bias between the two half-cells [70] or by integration of an artificial photosensitizer in the photoanode [71]. Although, most of the work published so far, is proof-of-concept studies and a real application is far from being realized, the basic concept opens various possibilities to study and optimize individual components and their interconnection. This knowledge may also guide the development of in vivo applications in future studies.

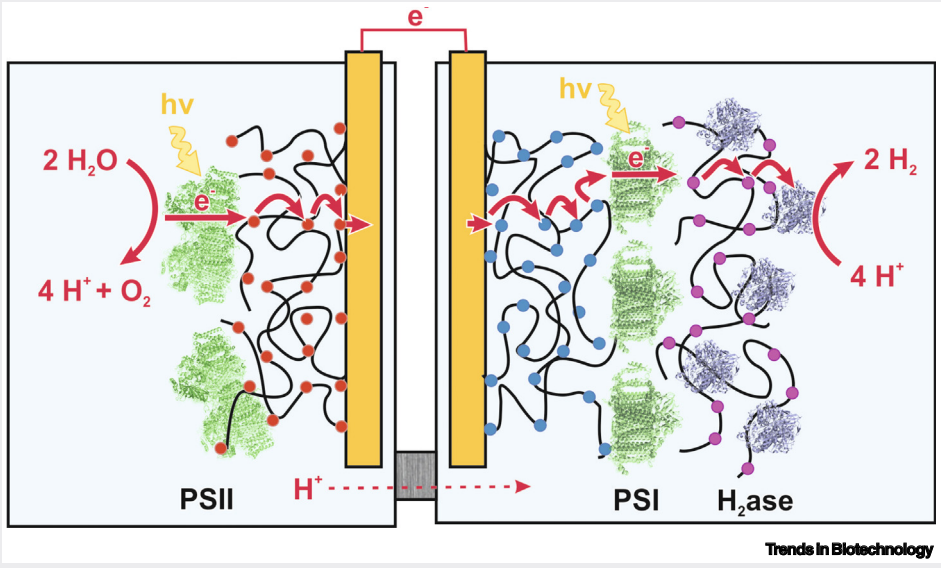

Figure I. Schematic model of a semiartificial photoelectrochemical cell. Electrons are released from water by photosystem (PS)II and transferred to the electrode via a redox active hydrogel in the anodic half-cell. Electron supply to PSI in the cathodic half-cell is mediated by a second hydrogel and a third hydrogel layer on top of PSI transfers the electrons to the embedded hydrogenase for hydrogen production at the end of the chain. Each hydrogel is modified with redox groups with a specific potential (indicated by colored circles) to enable diffusion-free electron transfer without additional bias.

Furthermore, it is promising for these approaches that the assembly of an active [FeFe]-hydrogenase has been shown to be possible without its maturation machinery *in vitro* as well as heterologously *in vivo* [45,46].

However, in many cases the longevity of *in vitro* systems is either poor or poorly characterized. Moreover, the hybrid nature of the systems lacks many of the advantages of a purely *in vivo* system: (i) cheap, fast, and nonlaborious assembly; (ii) production of biomass that can be repurposed for other uses (e.g., animal feed, biofuel, and water remediation); and (iii) the ability to be repaired and/or remade. However, insights from biohybrid *in vitro* and biological *in vivo* approaches have the potential to mutually guide the optimization of these processes.

Concluding remarks and future perspectives

The successful expression of PSI–H2ase fusions in a cyanobacterium and a green alga have been major steps towards sustainable biological light driven hydrogen production. The respective strains grow autotrophically and produce higher amounts of H_2 compared to their parent strains under the same conditions. For the time being, the algal system outcompetes the cyanobacterial one and sets an example for excellent electron transfer, but at the same time, it justifies the expectation that also cyanobacterial fusions could accomplish similar rates. The frequently mentioned lower turnover frequency of the [NiFe]-enzymes will not be limiting here since it is well sufficient for the *in vivo* electron flow through PSI [18,47].

One of the most obvious hurdles to overcome is the oxygen sensitivity of the algal [FeFe]- as well as the cyanobacterial [NiFe]-H_2ases. [NiFe]-enzymes should have an inherent advantage since all the enzymes of this class can be reactivated after oxygen exposure and oxygen-tolerant subclasses exist. In this respect, the recent successful expression of the oxygen-tolerant [NiFe]-H_2ase of the non-photosynthetic bacterium *Ralstonia eutropha* in the cyanobacterium *Synechocystis* sp. PCC 6803 is interesting although the enzyme expressed at low levels (~40 times less enzyme activity per mg of protein compared to its native host) and predominantly consumes H_2 [48].

In case of [FeFe]-H_2ases, oxygen sensitivity might be more difficult to overcome since no enzymes working in the presence of significant amounts of oxygen are known. However, recently [FeFe]-H_2ases were discovered that possess a safety cap, which protects the enzyme from degradation by O_2 but simultaneously inactivates the enzyme until O_2 concentrations drop [49]. It was also found that at least some (relatively) O_2-insensitive [FeFe]-H_2ases do not require additional domains for this property [50], making them candidates for the chimeric approach. These findings raise the hope that the space of biochemical properties of the [FeFe]-class has not been fully explored yet.

When photosynthetic light reaction is running, NADPH is formed by FNR from reduced Fdx and ATP is produced by ATP synthase using the proton gradient generated at the same time (Figure 1). Both products are consumed in a fixed ratio by the CBB cycle. When electron transfer to the hydrogenase is high, the amount of NADPH generated will drop. The overaccumulation of ATP (and resulting high proton motive force) will ultimately place a halt on electron transport. Thus, future efforts will need to focus on how to dissipate part of this gradient without harming the cells ATP requirements and viability.

Under high light intensities, photosynthetic cells usually absorb a higher proportion of the incident light than they can process. Consequently, they need many mechanisms to dissipate the surplus energy. To not waste this energy and to cover a wider range of photon flux densities, it will be necessary to minimize self-shading and decrease antenna size [51]. In addition, the limited spectral coverage of light harvesting could be expanded by introducing new antenna that absorb in until now untouched spectral regions [52,53].

One last obstacle that can be foreseen for sustained biological photoH_2 generation is the mesophilic nature of the model strains used until know. To enable technical scale production

Outstanding questions

How can oxygen resistance of the H_2ases be increased? More prospecting of H_2ases from the environment needs to be performed to identify hydrogenases with desired properties, such as oxygen tolerance and high catalytic rates in the direction of H_2 evolution. Although the chimeric studies started with the endogenous H_2ases, there is no reason why enzymes from other species cannot be used, as it is known that most maturases are capable of activating H_2ases from a range of species.

How can electron transfer inside the chimeric complexes be optimized? It will be important in the future to obtain actual structures of the chimeric assemblies, rather than relying upon models. Cryoelectron microscopy is a promising technique that has already been applied to PSI from both species, making it likely that structures can be obtained for PSI–HoxYH and PSI–HydA. Insights from these structures and from biohybrid *in vitro* approaches can guide the optimization of the complexes. The *in vitro* characterization of PSI–H_2ase chimeric complexes is furthermore a valuable tool to pinpoint and subsequently amend weak spots.

How can we ensure sustainability and viability of the cells? It is imperative to obtain a detailed understanding of the physiology of the engineered strains, the regulation of photosynthetic electron transport and the processes required for cell maintenance.

To have a real impact on sustainable photoH_2 production, how can the chimeric systems be moved to species better suited for industrial production? Although the species utilized here (*Synechocystis* and *Chlamydomonas*) have been used for decades as model systems, they are not ideal for large-scale cultivation. Given that PSI is highly conserved, however, there is no insurmountable obstacle to importing chimeric assemblies tested in model species into strains that have properties desirable for industrial scale-up (e.g., fast growth; tolerance to high light; extremophiles).

also under a wide temperature regime extremophilic strains and strains growing at high cell densities need to be used. However, the transfer of the necessary components should not be a large problem since the core of the photosynthetic apparatus and PSI is highly conserved among all oxygenic phototrophs (see Outstanding questions).

Acknowledgments

Funding is acknowledged from the German Ministry of Science and Education (BMBF: FP309), the German Science Foundation (DFG: GU1522/5-1, FOR2816/2, Research Training Group 2341 MiCon) and the U.S. National Science Foundation (CBET-1706960).

Declaration of interests

No interests are declared.

References

1. Ghirardi, M.L. *et al.* (2009) Photobiological hydrogen-producing systems. *Chem. Soc. Rev.* 38, 52–61
2. Milrad, Y. *et al.* (2018) Green algal hydrogenase activity is outcompeted by carbon fixation before inactivation by oxygen takes place. *Plant Physiol.* 177, 918
3. Cournac, L. *et al.* (2004) Sustained photoevolution of molecular hydrogen in a mutant of *Synechocystis* sp. Strain PCC 6803 deficient in the type I NADPH-dehydrogenase complex. *J. Bacteriol.* 186, 1737–1746
4. Kosourov, S. *et al.* (2018) A new approach for sustained and efficient H2 photoproduction by *Chlamydomonas reinhardtii*. *Energy Environ. Sci.* 11, 1431–1436
5. Kosourov, S. *et al.* (2020) Water oxidation by photosystem II is the primary source of electrons for sustained H2 photoproduction in nutrient-replete green algae. *Proc. Natl. Acad. Sci.* 117, 29629
6. Seefeldt, L.C. *et al.* (2020) Reduction of substrates by nitrogenases. *Chem. Rev.* 120, 5082–5106
7. Lindberg, P. *et al.* (2004) Gas exchange in the filamentous cyanobacterium Nostoc punctiforme strain ATCC 29133 and its hydrogenase-deficient mutant strain NHM5. *Appl. Environ. Microbiol.* 70, 2137–2145
8. Tsygankov, A.A. *et al.* (1999) H2 photoproduction by batch culture of *Anabaena variabilis* ATCC 29413 and its mutant PK84 in a photobioreactor. *Biotechnol. Bioeng.* 64, 709–715
9. Greening, C. *et al.* (2016) Genomic and metagenomic surveys of hydrogenase distribution indicate H2 is a widely utilised energy source for microbial growth and survival. *ISME J.* 10, 761–777
10. Lenz, O. *et al.* (2018) O(2)-tolerant [NiFe]-hydrogenases of *Ralstonia eutropha* H16: physiology, molecular biology, purification, and biochemical analysis. *Methods Enzymol.* 613, 117–151
11. Sawyer, A. and Winkler, M. (2017) Evolution of *Chlamydomonas reinhardtii* ferredoxins and their interactions with [FeFe]-hydrogenases. *Photosynth. Res.* 134, 307–316
12. Gutekunst, K. *et al.* (2014) The bidirectional NiFe-hydrogenase in *Synechocystis* sp. PCC 6803 is reduced by flavodoxin and ferredoxin and is essential under mixotrophic, nitrate-limiting conditions. *J. Biol. Chem.* 289, 1930–1937
13. McIntosh, C.L. *et al.* (2011) The [NiFe]-hydrogenase of the cyanobacterium *Synechocystis* sp. PCC 6803 works bidirectionally with a bias to H2 production. *J. Am. Chem. Soc.* 133, 11308–11319
14. Ash, P.A. *et al.* (2019) Unifying activity, structure, and spectroscopy of [NiFe] hydrogenases: combining techniques to clarify mechanistic understanding. *Acc. Chem. Res.* 52, 3120–3131
15. Caserta, G. *et al.* (2020) Hydroxy-bridged resting states of a [NiFe]-hydrogenase unraveled by cryogenic vibrational spectroscopy and DFT computations. *Chem. Sci.* 12, 2189–2197
16. Swanson, K.D. *et al.* (2015) [FeFe]-Hydrogenase oxygen inactivation is initiated at the H cluster 2Fe subcluster. *J. Am. Chem. Soc.* 137, 1809–1816
17. Lubitz, W. *et al.* (2014) Hydrogenases. *Chem. Rev.* 114, 4081–4148
18. Gutekunst, K. *et al.* (2018) *In-vivo* turnover frequency of the cyanobacterial NiFe-hydrogenase during photohydrogen production outperforms *in-vitro* systems. *Sci. Rep.* 8, 6083
19. Gutthann, F. *et al.* (2007) Inhibition of respiration and nitrate assimilation enhances photohydrogen evolution under low oxygen concentrations in *Synechocystis* sp. PCC 6803. *Biochim. Biophys. Acta (BBA) Bioenerg.* 1767, 161–169
20. Boichenko, V.A. *et al.* (2004) Hydrogen production by photosynthetic microorganisms. In *Molecular to Global Photosynthesis*, pp. 397–451, Imperial College Press
21. Melis, A. *et al.* (2000) Sustained photobiological hydrogen gas production upon reversible inactivation of oxygen evolution in the green alga *Chlamydomonas reinhardtii*. *Plant Physiol.* 122, 127–136
22. Steinbeck, J. *et al.* (2015) Deletion of proton gradient regulation 5 (PGR5) and PGR5-like 1 (PGRL1) proteins promote sustainable light-driven hydrogen production in *Chlamydomonas reinhardtii* due to increased PSII activity under sulfur deprivation. *Front. Plant Sci.* 6, 892
23. Scoma, A. *et al.* (2014) Acclimation to hypoxia in *Chlamydomonas reinhardtii*: can biophotolysis be the major trigger for long-term H2 production? *New Phytol.* 204, 890–900
24. Ben-Zvi, O. *et al.* (2019) Re-routing photosynthetic energy for continuous hydrogen production in vivo. *Biotechnol. Biofuels* 266
25. Marco, P. *et al.* (2019) Binding of ferredoxin NADP(+) oxidoreductase (FNR) to plant photosystem I. *Biochim. Biophys. Acta Bioenerg.* 1860, 689–698
26. Rumpel, S. *et al.* (2014) Enhancing hydrogen production of microalgae by redirecting electrons from photosystem I to hydrogenase. *Energy Environ. Sci.* 7, 3296–3301
27. Wiegand, K. *et al.* (2018) Rational redesign of the ferredoxin-NADP+-oxido-reductase/ferredoxin-interaction for photosynthesis-dependent H2-production. *Biochim. Biophys. Acta BBA Bioenerg.* 1859, 253–262
28. Yacoby, I. *et al.* (2011) Photosynthetic electron partitioning between [FeFe]-hydrogenase and ferredoxin:NADP+-oxidoreductase (FNR) enzymes *in vitro*. *Proc. Natl. Acad. Sci.* 108, 9396–9401
29. Eilenberg, H. *et al.* (2016) The dual effect of a ferredoxin-hydrogenase fusion protein in vivo: successful divergence of the photosynthetic electron flux towards hydrogen production and elevated oxygen tolerance. *Biotechnol. Biofuels* 9, 182
30. Nagy, V. *et al.* (2018) Water-splitting-based, sustainable and efficient H2 production in green algae as achieved by substrate limitation of the Calvin–Benson–Bassham cycle. *Biotechnol. Biofuels* 11, 69
31. Burlacot, A. *et al.* (2018) Flavodiiron-mediated O(2) photoreduction links H(2) production with CO(2) fixation during the anaerobic induction of photosynthesis. *Plant Physiol.* 177, 1639–1649
32. Jokel, M. *et al.* (2019) Elimination of the flavodiiron electron sink facilitates long-term H2 photoproduction in green algae. *Biotechnol. Biofuels* 12, 280
33. Valladares, A. *et al.* (2003) Cytochrome c oxidase genes required for nitrogenase activity and diazotrophic growth in *Anabaena* sp. PCC 7120. *Mol. Microbiol.* 47, 1239–1249
34. Avilan, L. *et al.* (2018) Phototrophic hydrogen production from a clostridial [FeFe] hydrogenase expressed in the heterocysts of

the cyanobacterium *Nostoc* PCC 7120. *Appl. Microbiol. Biotechnol.* 102, 5775–5783
35. Roumezi, B. *et al.* (2020) Overproduction of the Flv3B flavodiiron, enhances the photobiological hydrogen production by the nitrogen-fixing cyanobacterium Nostoc PCC 7120. *Microb. Cell Factories* 19, 65
36. Appel, J. *et al.* (2020) Cyanobacterial *in vivo* solar hydrogen production using a photosystem I–hydrogenase (PsaD-HoxYH) fusion complex. *Nat. Energy* 5, 458–467
37. Kanygin, A. *et al.* (2020) Rewiring photosynthesis: a photosystem I-hydrogenase chimera that makes H2 *in vivo*. *Energy Environ. Sci.* 13, 2903–2914
38. Parrett, K.G. *et al.* (1989) Purification and properties of the intact P-700 and Fx-containing Photosystem I core protein. *Biochim. Biophys. Acta* 973, 324–332
39. Page, C.C. *et al.* (1999) Natural engineering principles of electron tunnelling in biological oxidation–reduction. *Nature* 402, 47–52
40. Takahashi, Y. *et al.* (1991) Directed chloroplast transformation in *Chlamydomonas reinhardtii*: insertional inactivation of the psaC gene encoding the iron sulfur protein destabilizes photosystem I. *EMBO J.* 10, 2033–2040
41. Redding, K. *et al.* (1998) A systematic survey of conserved histidines in the core subunits of Photosystem I by site-directed mutagenesis reveals the likely axial ligands of P700. *EMBO J.* 17, 50–60
42. Meimberg, K. *et al.* (1999) Lys35 of PsaC is required for the efficient photoreduction of flavodoxin by photosystem I from *Chlamydomonas reinhardtii*. *Eur. J. Biochem.* 263, 137–144
43. Ihara, M. *et al.* (2006) Light-driven hydrogen production by a hybrid complex of a [NiFe]-hydrogenase and the cyanobacterial photosystem I. *Photochem. Photobiol.* 82, 676–682
44. Krassen, H. *et al.* (2009) Photosynthetic hydrogen production by a hybrid complex of photosystem I and [NiFe]-hydrogenase. *ACS Nano* 3, 4055–4061
45. Berggren, G. *et al.* (2013) Biomimetic assembly and activation of [FeFe]-hydrogenases. *Nature* 499, 66–69
46. Wegelius, A. *et al.* (2018) Generation of a functional, semisynthetic [FeFe]-hydrogenase in a photosynthetic microorganism. *Energy Environ. Sci.* 11, 3163–3167
47. Theune, M.L. *et al.* (2021) *In-vivo* quantification of electron flow through photosystem I – Cyclic electron transport makes up about 35% in a cyanobacterium. *Biochim. Biophys. Acta (BBA) Bioenerg.* 1862, 148353
48. Lupacchini, S. *et al.* (2021) Rewiring cyanobacterial photosynthesis by the implementation of an oxygen-tolerant hydrogenase. *Metab. Eng.* 68, 199–209
49. Winkler, M. *et al.* (2021) A safety cap protects hydrogenase from oxygen attack. *Nat. Commun.* 12, 756
50. Caserta, G. *et al.* (2018) Engineering an [FeFe]-hydrogenase: do accessory clusters influence O(2) resistance and catalytic bias? *J. Am. Chem. Soc.* 140, 5516–5526
51. Croce, R. and van Amerongen, H. (2020) Light harvesting in oxygenic photosynthesis: Structural biology meets spectroscopy. *Science* 369, eaay2058
52. Slattery, R.A. and Ort, D.R. (2021) Perspectives on improving light distribution and light use efficiency in crop canopies. *Plant Physiol.* 185, 34–48
53. Tros, M. *et al.* (2020) Harvesting far-red light: functional integration of chlorophyll f into Photosystem I complexes of *Synechococcus* sp. PCC 7002. *Biochim. Biophys. Acta Bioenerg.* 1861, 148206
54. Gorbunov, M.Y. and Falkowski, P.G. (2021) Using chlorophyll fluorescence to determine the fate of photons absorbed by phytoplankton in the world's oceans. *Annu. Rev. Mar. Sci.* 4, 213–238
55. Torzillo, G. and Seibert, M. (2013) Hydrogen production by *Chlamydomonas reinhardtii*. In *Handbook of Microalgal Culture*, pp. 417–432, Wiley–Blackwell
56. Redding, K. and van der Est, A. (2006) The Directionality of electron transfer in photosystem I. In *Photosystem I: The Plastocyanin: Ferredoxin Oxidoreductase in Photosynthesis* (Golbeck, J., ed.), pp. 413–437, Kluwer Academic Publishers
57. Müller, M.G. *et al.* (2010) Independent initiation of primary electron transfer in the two branches of the photosystem I reaction center. *Proc. Natl. Acad. Sci. U. S. A.* 107, 4123–4128
58. Byrdin, M. *et al.* (2006) Assignment of a kinetic component to electron transfer between iron-sulfur clusters F_X and $F_{A/B}$ of Photosystem I. *Biochim. Biophys. Acta* 1757, 1529–1538
59. Moser, C.C. *et al.* (1992) Nature of biological electron transfer. *Nature* 355, 796–802
60. Peters, J.W. *et al.* (1998) X-ray crystal structure of the Fe-only hydrogenase (CpI) from Clostridium pasteurianum to 1.8 angstrom resolution. *Science* 282, 1853–1858
61. Plumeré, N. and Nowaczyk, M.M. (2016) Biophotoelectrochemistry of photosynthetic proteins. *Adv. Biochem. Eng. Biotechnol.* 158, 111–136
62. Ruff, A. *et al.* (2020) Bioelectrocatalysis as the basis for the design of enzyme-based biofuel cells and semi-artificial biophotoelectrodes. *Nat. Catal.* 3, 214–224
63. Kothe, T. *et al.* (2013) Combination of a photosystem 1-based photocathode and a photosystem 2-based photoanode to a z-scheme mimic for biophotovoltaic applications. *Angew. Chem. Int. Ed.* 52, 14233–14236
64. Zhao, F. *et al.* (2019) A photosystem I monolayer with anisotropic electron flow enables Z-scheme like photosynthetic water splitting. *Energy Environ. Sci.* 12, 3133–3143
65. Robinson, M.T. *et al.* (2017) Mediated approaches to photosystem I-based biophotovoltaics. *Curr. Opin. Electrochem.* 5, 211–217
66. Badura, A. *et al.* (2011) Wiring photosynthetic enzymes to electrodes. *Energy Environ. Sci.* 4, 3263–3274
67. Wang, P. *et al.* (2021) Closing the gap for electronic short-circuiting: photosystem i mixed monolayers enable improved anisotropic electron flow in biophotovoltaic devices. *Angew. Chem. Int. Ed.* 60, 2000–2006
68. Ruff, A. (2017) Redox polymers in bioelectrochemistry: common playgrounds and novel concepts. *Curr. Opin. Electrochem.* 5, 66–73
69. Zhao, F. *et al.* (2015) Light induced H2 evolution from a biophotocathode based on photosystem 1 – Pt nanoparticles complexes integrated in solvated redox polymers films. *J. Phys. Chem. B* 119, 13726–13731
70. Mersch, D. *et al.* (2015) Wiring of photosystem II to hydrogenase for photoelectrochemical water splitting. *J. Am. Chem. Soc.* 137, 8541–8549
71. Sokol, K.P. *et al.* (2018) Bias-free photoelectrochemical water splitting with photosystem II on a dye-sensitized photoanode wired to hydrogenase. *Nat. Energy* 3, 944–951
72. Lubner, C.E. *et al.* (2011) Solar hydrogen-producing bionanodevice outperforms natural photosynthesis. *Proc. Natl. Acad. Sci. U. S. A.* 108, 20988–20991